Current Research Journal of Biological Sciences 2(2): 83-102, 2010
ISSN: 2041-0778

Submitted Date: July 11, 2009 Accepted Date: July 24, 2009 Published Date: March 10, 2010

Molecular Modeling Evaluation of the Antimalarial Activity of Artemisinin Analogues: Molecular Docking and Rescoring using Prime/MM-GBSA Approach

Mani Srivastava, Harvinder Singh and Pradeep Kumar Naik
Department of Bioinformatics and Biotechnology, Jaypee University of Information Technology, Waknaghat, Solan 173215, Himachal Pradesh, India

Abstract: Artemisinin, a class of sesquiterpene endoperoxide, has been the objective of numerous studies to prepare better and safer anti-malarial drugs. A library of artemisinin analogues has been designed consisting of 144 analogues. The combined approaches of docking-molecular mechanics based on generalized Born/surface area (MM-GBSA) solvation model showed that artemisinin and its structural derivatives approach haem by pointing O1 and O2 at the endoperoxide linkage toward the iron center, a mechanism that is controlled by steric hindrance. A linear correlation was observed between the O-Fe distance and Glide score and binding free energy with correlation coefficient (R^2) of 0.658 and 0.707. Quantitative structure activity relationships were developed between the anti-malarial activity (pIC_{50}) of these compounds and molecular descriptors like docking score and binding free energy. Using Glide score and binding free energy the R^2 were found in the range of 0.763 to 0.734 and 0.718 to 0.786 indicating that the predictive capabilities of the models were acceptable. Low level of root means square error for the majority of inhibitors which establish the docking and prime/MM-GBSA based prediction model as an efficient tool for generating more potent and specific inhibitors of haem by testing rationally designed lead compounds based on artemisinin derivatives.

Key words: Artemisinin, molecular docking, prime/MM-GBSA, virtual screening

INTRODUCTION

Malaria is one of the most common diseases in tropical countries. Over 300 million new malaria infections and millions of deaths due to malaria occur worldwide each year. The rapid spread of resistance to current quinoline anti-malarial has made malaria a major global problem. Because a vaccine for malaria is not available, it is essential to find new anti-malarial drugs and understand their anti-malarial mechanism for treating patients.

Artemisinin (qinghaosu), a sesquiterpene endoperoxide isolated from *Artemisia annua,* is a remarkable life saving anti-malarial compound, effective against drug-resistant *Plasmodium falciparum* and cerebral malaria (Klayman, 1985; Jung, 1994; Zhou and Xu, 1994; Haynes and Vonwiller, 1996; Cumming *et al*., 1997). Artemisinin and its derivatives induce more rapid reduction of parasitemia decreasing the number of parasites faster than any other known drugs. As a consequence they are of special interest for severe malaria. The first decline in the number of parasites is also beneficial for combination therapies. Artemisinin has a unique structure (Fig. 1a) bearing a stable endoperoxide lactone (1, 2, 4-trioxane) totally different from previous anti-malarial in its structure and mode of action. This has led to tremendous interest in the mechanism of action (Cumming *et al*., 1997), chemistry (Haynes and Vonwiller, 1996) and drug development (Jung, 1994) of this novel class of anti-malarial. The peroxide group is essential for anti-malarial activity (Klayman, 1985) and is mediated by activated oxygen (superoxide, H_2O_2 and/or hydroxyl radicals) or carbon free-radicals (Mishnick *et al*., 1993; Cumming *et al*., 1997). This is evident from the inactivity of the deoxyartemisinin compound (Fig. 1b) that lacks the endoperoxide moiety China Cooperative Research group (1982). The high selectivity in the killing of parasites by artemisinin may be due to its interaction (Meshnick *et al*., 1991) with haem which accumulates in high quantities in parasitized red blood cells as a by-product of haemoglobin lysis by the malarial parasite (Goldberg, 1990). Since free haem is toxic to the parasite, it is sequestered by oxidative polymerization by the parasite to a non-toxic and insoluble material called haemozoin which accumulates as a crystalline pallet in the cytosol of the erythrocytes (Goldberg, 1990). From studies with model systems, Jefford *et al.* (1996) suggested that 1,2,4-trioxanes structurally related to artemisinin form a complex with Fe (II) of haem and generate oxyl radicals, whereas Posner *et al* (1996) proposed that Fe-catalyzed decomposition of artemisinin leads to reactive carbon centered free radicals, high valent iron–oxo species, and electrophiles. The chemical behavior of artemisinin in the presence of haem and non-haem Fe (II) and Fe (III) has been studied and artemisinin decomposition products of such reactions have been identified by Haynes and Vonwiller (1996).

Corresponding Author: Pradeep Kumar Naik, Department of Bioinformatics and Biotechnology, Jaypee University of Information Technology, Waknaghat, Solan 173215, Himachal Pradesh, India
Ph: +91-1792-239227 Fax: +91-1792-245362

Prompted by the clinical successes of the artemisinin, significant efforts have been focused on identifying new analogues that have a similar mechanism of action yet superior in activity. A consistent number of structural modifications have been introduced in the original structure of artemisinin in order to overcome the solubility as well as neurotoxic problem associated with its utilization as anti-malarial drug. The study and assessment of these have permitted the clinical development and their usage in the treatment of malaria. Since the discovery of the therapeutic properties of artemisinin, new findings related to its activities, its mechanism of action and pharmacological properties, have been unveiled. The great diversity of the artemisinin analogues, the huge number of assays carried out on them and the different mechanisms of action observed in the different series make it difficult to clearly define the minimum structural requirements necessary for their biological activity. Additionally, the results available have been obtained by different authors, at different times using different technologies and on very diverse types of cell lines. For all these reasons, greater systematization would be required to obtain definitive conclusions. The mechanism of action of any drug is very important in drug development. Generally, the drug compound binds with a specific target, a receptor, to mediate its effects. Therefore, suitable drug receptor interactions are required for high activity. Understanding of the nature of these interactions is very significant and in theoretical calculations in particular, the molecular docking method seem to be a proper tool for gaining such understanding. The docking results obtained will give information on how the chemical structure of the drug should be modified to achieve suitable interactions and for the rapid prediction and virtual prescreening of anti-malarial activity.

The process of structure-based design started with the detailed analysis of binding site of the target protein, preferably in its complex form with a ligand. The knowledge of binding site helps design novel drug candidates with better potency. Another approach that uses the structural information deals with the protein-based virtual screening of chemical databases. Whereas prior to biological screening the potent compounds are computationally figured out from a large chemical library. Docking methods have the added advantage compared to 2-D similarity and 3-D pharmacophore search methods because it makes use of 3-D receptor structure in a quantitative way. Compound selection based on docking calculations alone and/or combined with virtual screening has been carried out for targets thrombin (Massova *et al.*, 1998), thymidylate synthase (Shoichet *et al.*, 1993), dihydrofolate reductase (Gschwend *et al.*, 1997), HIV protease (Friedman *et al.*, 1998), PTP1B (Doman *et al.*, 2002), human carbonic anhydrase (Gruneberg *et al.*, 2002) and such study led to the identification of novel compounds with the potency between 1-100 µM.

In this study we created a virtual library of artemisinin analogues which are collected from different sources and their mode of interaction and binding affinity with haem have been evaluated. Further, prediction models for predicting the anti-malarial activity of these compounds were developed based on docking score and binding free energy as molecular descriptors. These prediction models were used for predicting the anti-malarial activity of newly developed analogues. We have used the molecular modeling techniques (molecular docking and rescoring using Prime/MM-GBSA) to find the series of artemisinin analogues that should be modified for energetically favorable interaction with haem and for better anti-malarial activity.

MATERIALS AND METHODS

Receptor preparation: The X-ray structure of haem-pdb was taken from the Protein Data Bank (PDB ID: 1CTJ) and has been used as initial structure in the preparation of haem receptor site. Haem is a planar molecule with a strong positive charge on its central iron atom, which lies slightly above the porphyrin plane (Fig. 1c). Charge on the iron was assigned as +2 but the structure was kept the same. Hydrogen was added to the model automatically via the Maestro interface leaving no lone pair and using an explicit all-atom model. The multi step Schrodinger's protein preparation tool (PPrep) has been used for final preparation of receptor model. The structure was energy minimized using OPLS 2005 force field and the conjugate gradient algorithm, keeping all atoms except hydrogen fixed. The minimization was stopped either after 1000 steps or after the energy gradient converged below 0.01 KJ/mol. Complete geometry optimization was carried out using LACVP** (Hay and Wadt, 1985) for the iron atoms, followed by single-point calculations using LACV3P** (Hay and Wadt, 1985) for the iron atom. Unrestricted density functional theory (DFT) was employed to effectively model the open shell orbital on the two iron atoms. The Jaguar suite of ab initio quantum chemical program Jaguar (Schrodinger Inc.) was used to carry out all quantum mechanics (QM) calculations.

Preparation of ligands: An initial dataset of 144 artemisinin analogues were collected from published data (Lin *et al.*, 1989; Posner *et al.*, 1992; Acton *et al.*, 1993; Avery *et al.*, 1995; Avery *et al.*, 1996; Pinheiro *et al.*, 2001) in which several different ring systems were represented. All of the analogues were either peroxides or trioxanes which acted via similar mechanism of action and were categorized into 9 classes (Table 1). Each of these compounds associated *in vitro* bioactivity values (IC_{50} values reported in ng/ml) against the drug resistant malaria strain *P. falciparum* (W-2 clone). The log value of the relative activity (RA) of these compounds was used for analysis and was defined as:

Table 1a: Artemisinin analogues with antimalarial activities against the drug-resistant malarial strain *P. falciparum* (W-2 clone) used in the study

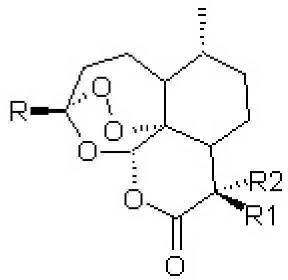

(1-24)

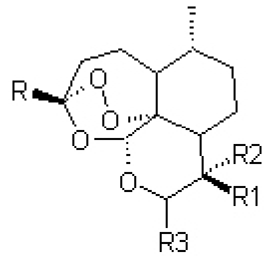

(25-62)

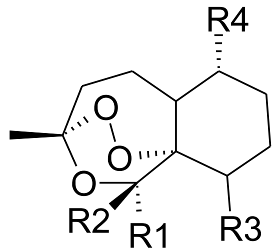

(63-74)

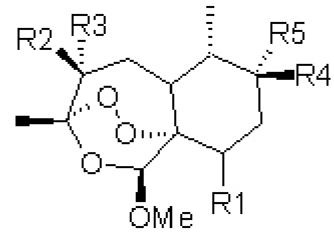

(75-79)

Compounds	R	R1	R2	R3	R4	R5	log (RA)	IC_{50} (ng/ml)
1	CH_3	CH_3	H				1.00	0.040
2	C_4H_8Ph	H	H				0.45	0.194
3	CH_3	H	2-Z-Butenyl				- 1.10	5.750
4	CH_3	H	H				0.79	0.065
5	CH_3	Allyl	H				0.34	0.550
6	CH_3	C_4H_9	H				0.17	0.311
7	C_4H_8Ph	C_4H_9	H				- 0.32	1.310
8	$CH_2CH_2CO_2Et$	C_4H_9	H				1.36	0.025
9	C_4H_9	C_4H_9	H				- 0.48	1.568
10	CH_3	C_2H_5	H				1.40	0.017
11	CH_3	C_6H_{13}	H				0.86	0.069
12	CH_3	i- C_6H_{13}	H				- 0.04	0.547
13	CH_3	i-C_5H_{11}	H				0.07	0.408
14	C_3H_6(p-Cl-Ph)	H		H			0.10	0.457
15	C_4H_9	H		H			- 0.74	2.416
16	$CH_2CH_2CO_2Et$	H		H			0.37	0.214
17	CH_3	C_3H_6(p-Cl-Ph)	H				1.37	0.025
18	CH_3	Br	CH_2	Br			- 1.64	27.24
19	CH_3	$=CH_2$	-				- 0.89	3.083
20	CH_3	CH_2CH_3	-				- 0.36	1.053
21	CH_3	$-CH_2CH_2-$	-				- 0.94	3.632
22	CH_3	C_5H_{11}	H				1.02	0.046
23	CH_3	C_4H_8Ph	H				0.63	0.133
24	CH_3	C_4H_8Ph	H				0.12	0.400
25	CH_3	CH_3	H	H			0.75	0.068
26	CH_3	CH_3	H	OH			0.55	0.114
27	CH_3	CH_3	H	OEt			0.34	0.202
28	CH_3	CH_3	H	OH			0.96	0.051
29	CH_3	H	Br	H			0.28	0.248
30	CH_3	CH_3	Br	NH-2-(1,3-thiazole)			0.66	0.134
31	CH_3	CH_3	Br	p-Cl-aniline			0.79	0.105
32	CH_3	CH_3	Br	aniline			0.18	0.397
33	CH_3	Br	CH_3	NH-2-pyridine			- 0.09	0.768
34	CH_3	CH_3	Br	NH-2-pyridine			- 0.77	3.667
35	CH_3	CH_3	H	α -OEt			0.32	0.212
36	CH_3	C_4H_9	H	H			1.32	0.021
37	CH_3	C_2H_5	H	H			0.67	0.086
38	CH_3	C_3H_7	H	OEt			- 0.04	0.529
39	CH_3	H	H	OEt			0.43	0.157
40	CH_3	CH_3	H	C_3H_6OH			0.78	0.077
41	CH_3	CH_3	H	C_4H_9			0.06	0.400
42	CH_3	CH_3	H	OCH_2CO_2Et			0.52	0.158
43	CH_3	CH_3	H	$OC_2H_4CO_2Me$			0.10	0.433
44	CH_3	CH_3	H	$OC_3H_6CO_2Me$			- 0.03	0.605
45	CH_3	CH_3	H	OCH_2 (4-PhCO_2Me)			- 0.07	0.720
46	CH_3	CH_3	H	(R)-$OCH_2CH(CH_3)CO_2Me$			1.79	0.009
47	CH_3	CH_3	H	(S)-$OCH_2CH(CH_3)CO_2Me$			2.25	0.003
48	CH_3	CH_3	H	(R)- $OCH(CH_3)CH_2CO_2Me$			0.87	0.073
49	CH_3	CH_3	H	(S)-$OCH(CH_3)CH_2CO_2Me$			1.70	0.011
50	$CH_2CH_2CO_2Et$	H	H	H			0.70	0.096
51	C_4H_9	H	H	H			0.75	0.075
52	C_4H_8Ph	H	H	H			0.58	0.139
53	CH_3	$-OCH_2-$	-	OOH			- 0.62	1.857
54	CH_3	$-CH_2O-$	-	OOH			- 0.57	1.655
55	CH_3	$=CH_2$	-	OOH			- 0.99	4.131
56	CH_3	C_5H_{11}	H	H			0.16	0.318
57	CH_3	C_3H_6Ph	H	H			1.40	0.021
58	CH_3	CH_3	H	Oot-C_4H_9			0.92	0.061
59	-	CH_3	OH	α-OH			- 0.89	3.303
60	-	CH_3	H	CH_2CHF_2			0.11	0.366
61	-	CH_3	OH	OCH_2CF_3			0.33	0.243
62	-	CH_3	OH	OEt			- 0.44	1.281
63		O CH_2Ph	H	H	H		- 0.09	0.530

Table 1: (Continued)

Compounds	R	R1	R2	R3	R4	R5	log (RA)	IC_{50} (ng/ml)
64		O CH_3	H	$C_2H_4O_2CNEt$	H		- 0.65	0.118
65		H	O CH_3	$C_2H_4OCH_3$	H		- 0.39	0.996
66		H	O CH_3	$C_2H_4OCH2Ph$	H		0.75	0.091
67		H	O CH_3	C_2H_4O-allyl	H		0.40	0.184
68		H	O CH_3	$C_2H_4O_2Ph$	H		- 0.59	2.086
69		H	O CH_3	$C_2H_4O_2C(4\text{-}PhCO_2Me)$	H		0.27	0.343
70		H	O CH_3	$C_2H_4O_2C(4\text{-}PhCO_2H)$	H		- 0.81	3.856
71		-	O CH_3	-	-		1.70	0.398
72		H	O CH_3	$C_2H_4O_2C(4\text{-}PhCO_2C_2H_4NMe_2)$	H		0.25	2.790
73		H	O CH_3	$C_2H_4O_2CCH_2NCO_2\text{-}(t\text{-}C_2H_9)$	H		- 0.04	0.670
74		H	O CH_3	$C_2H_4OCH_2$ (4-N-Me-pyridine)	H		- 0.90	4.439
75		C_2H_4OH	H	CH_3	H	H	- 1.80	26.849
76		C_2H_4OH	CH_3	H	H	H	0.23	0.251
77		C_2H_4OH	CH_3	CH_3	H	H	- 1.80	28.102
78		$C_2H_4OCH_2Ph$	CH_3	CH_3	H	H	- 1.80	36.157
79		$C_2H_4OCH_2$(4-py)	-	-	-	-	0.14	0.373

Table 1b: (Continued): Miscellaneous artemisinin analogues with antimalarial activities against the drug-resistant malarial strain *P. falciparum* (W-2 clone) used in the study

Compounds	Structure	log (RA)	IC_{50} (ng/ml)
80	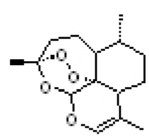	0.78	0.063
81	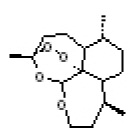	-1.20	6.340
82	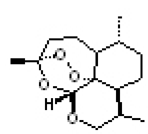	-0.79	2.344
83	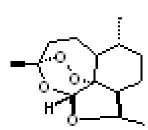	-0.64	1.573
84	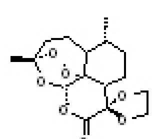	-2.09	56.889
85	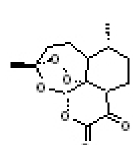	-2.49	123.612

Table 1: (Continued)

Compounds	Structure	log (RA)	IC_{50} (ng/ml)
86	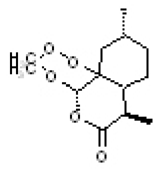	- 0.800	2.309
87	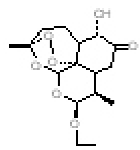	0.160	0.320
88	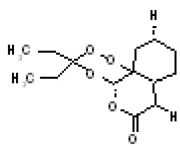	- 0.600	1.525
89	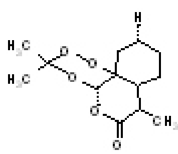	- 1.270	6.762
90	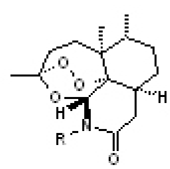	0.328	0.400
91	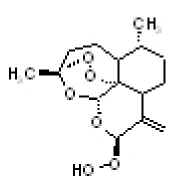	- 0.739	2.320
92	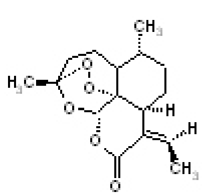	- 0.197	0.657

Table 1: (Continued)

Compounds	Structure	log (RA)	IC_{50} (ng/ml)
93	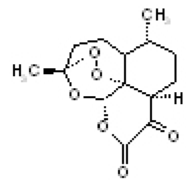	- 2.298	79.429
94	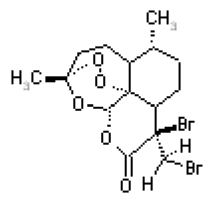	- 1.487	19.143
95	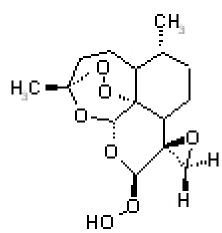	- 0.460	1.286
96	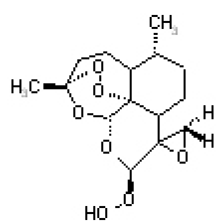	- 0.409	1.143
97	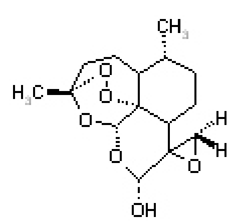	- 0.361	0.971

Table 1c: (Continued) Dihydroartemisinin derivatives with antimalarial activities against the drug-resistant malarial strain *P. falciparum* (W-2 clone) used in the study

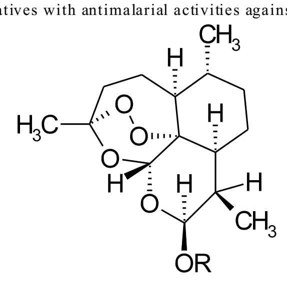

Compounds	R	log (RA)	IC_{50} (ng/ml)
98	OR = H	0.487	0.123
99	(S)-$CH_2CH(CH_3)COOCH_3$	2.104	0.004
100	(S)-$CH(CH_3)CH_2COOCH_3$	0.599	0.137
101	1-adamantylmethyl	0.007	0.020
102	(S)-$CH_2CH(CH_3)COOH$	- 0.658	0.603
103	(S)- $CH(CH_3)CH_2COOH$	- 0.608	2.123
104	(R)-$CH(CH_3)CH_2COOH$	- 0.383	2.380
105	OR= =O-	0.269	0.743
106	$CH_2PhCOOH$	0.176	0.394
107	(R)-$CH_2CH(CH_3)COOCH_3$	1.524	0.016
108	(R)-$CH_2CH(CH_3)COOH$-	0.463	1.520

Table 1d: (Continued): Tricyclic 1, 2, 4 – trioxanes derivatives with antimalarial activities against the drug-resistant malarial strain *P. falciparum* (W-2 clone) used in the study

Compounds	Structure	log (RA)	IC_{50} (ng/ml)
109	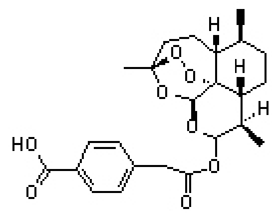	- 0.475	1.886
110	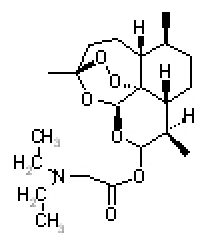	0.995	0.057
111	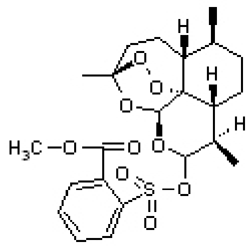	- 0.413	1.771
112	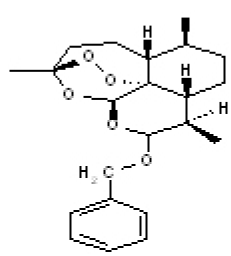	0.968	0.057

Table 1: (Continued)

Compounds	Structure	log (RA)	IC_{50} (ng/ml)
113	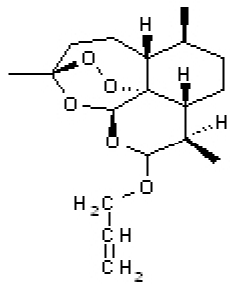	0.905	0.057
114	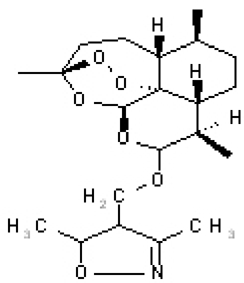	0.991	0.057
115	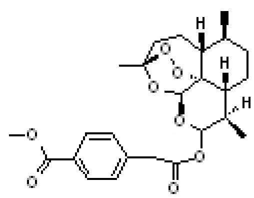	0.660	0.143
116	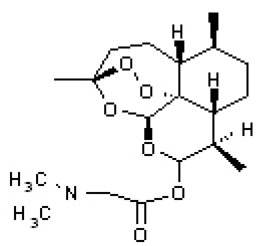	0.787	0.086
117	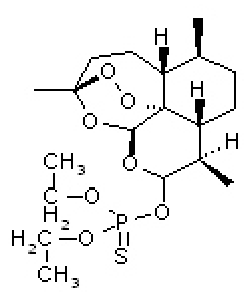	0.717	0.057

Table 1: (Continued)

Compounds	Structure	log (RA)	IC_{50} (ng/ml)
118	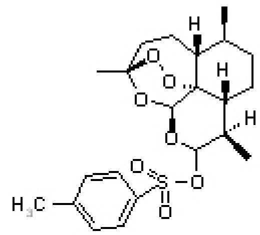	0.434	0.229
119	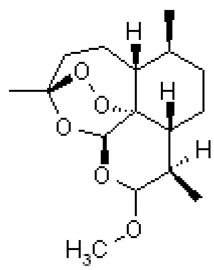	0.129	0.314

Table 1e: (Continued): 3C- substituted artemisinin derivatives with antimalarial activities against the drug-resistant malarial strain *P. falciparum* (W-2 clone) used in the study

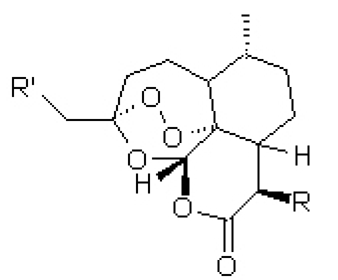

Compounds	R1	R	log (RA)	IC_{50} (ng/ml)
120	CH_3	H	0.049	0.357
121	CH_3 CH_2	H	0.828	0.062
122	CH_3CH	H	- 0.347	0.977
123	EtO_2CCH_2	H	0.365	0.216
124	$C_6H_5CH_2$	H	- 2.000	50.78
125	p-$ClC_6H_4(CH_2)_2$	-	0.104	0.453
126	C_6H_5 $(CH_2)_3$	H	0.449	0.195
127	CH_3	CH_3 $(CH_2)_3$	0.410	0.187
128	$CH_3(CH_2)_2$	CH_3 $(CH_2)_3$	- 0.481	1.573
129	$C_6H_5CH_2$	$CH_3(CH_2)_3$	- 2.000	58.72
130	p-$ClC_6H_4(CH_2)_2$	CH_3 $(CH_2)_3$	- 0.276	1.239
131	$C_6H_5(CH_2)_3$	CH_3 $(CH_2)_3$	- 0.319	1.306
132	EtO_2CCH_2	$CH_3(CH_2)_3$	1.359	0.025

Table 1f: (Continued): Deoxy artemisinin derivatives with antimalarial activities against the drug-resistant malarial strain *P. falciparum* (W-2 clone) used in the study

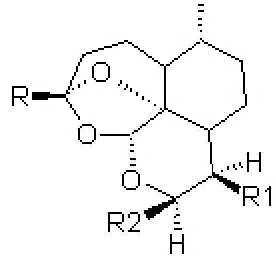

Compounds	R	R1	R2	log (RA)	IC_{50} (ng/ml)
133	CH_3	CH_3	OEt	-4	4198.58
134	CH_3	CH_3	OH	-4	3801.42
135	CH_3	C_4H_8Ph	-	-4	5248.23
136	CH_3	C_3H_7	-	-4	3971.63
137	CH_3	CH_3	-	-4	4567.37
138	CH_3	C_4H_9	H	-4	4170.21
139	$CH_2CH_2CO_2Et$	H	H	-4	4652.48
140	C_2H_4Ph	H	-	-4	3574.47
141	CH_2CH_3	H	-	-4	3574.47
142	CH_3	C_2H_4Ph	-	-4	4851.06
143	CH_3	C_3H_6Ph	-	-4	5049.64
144	CH_3	CH_3	-	-4	3773.05

Table 2: Experimental and theoretical values of the 1,2,4-trioxane ring parameters in artemisinin (bond lengths in Å; bond angles and torsional angles in degrees)

	Theoretical			Experimental[d]	Experimental[e]
Parameters[a]	3-21G[b]	3-21G**[c]	6-31G[c]		
O1-O2	001.463	001.462	001.447	001.475(4)	001.469(2)
O2-C3	001.441	001.440	001.435	001.417(4)	001.416(3)
C3-O4	001.436	001.436	001.435	001.448(4)	001.445(2)
O4-C5	001.407	001.408	001.403	001.388(4)	001.379(2)
C5-C6	001.529	001.530	001.533	001.528(5)	001.523(2)
C6-O1	001.478	001.477	001.469	001.450(4)	001.461(2)
O1-O2-C3	106.900	107.070	108.800	107.600(2)	108.100(1)
O2-C3-O4	107.000	107.310	106.760	107.200(2)	106.600(2)
C3-O4-C5	115.600	115.700	117.300	113.500(3)	114.200(2)
O4-C5-C6	112.000	112.030	112.280	114.700(2)	114.500(2)
C5-C6-O1	111.100	111.589	110.910	111.100(2)	110.700(2)
C6-O1-O2	111.200	111.286	113.240	111.500(2)	111.200(2)
O1-O2-C3-O4	- 074.900	- 074.680	- 071.840	- 075.500(3)	- 075.500(2)
O2-C3-O4-C5	031.800	032.150	033.390	036.300(4)	036.000(2)
C3-O4-C5-C6	029.400	028.400	025.320	024.800(4)	025.300(2)
O4-C5-C6-O1	- 051.800	- 050.769	- 049.410	- 050.800(4)	- 051.300(2)
C5-C6-O1-O2	010.100	009.792	012.510	012.300(3)	012.700(2)
C6-O1-O2-C3	050.800	050.522	046.700	047.700	047.800(2)

[a] Atoms are numbered according to Fig. 1
[b] Present study
[c] Values from Leban *et al.* (1988)
[d] Values from Fersht (1984) (experimental estimated standard deviations in brackets)
[e] Values from Lisgarten *et al.* (1998) (experimental estimated standard deviations in brackets)

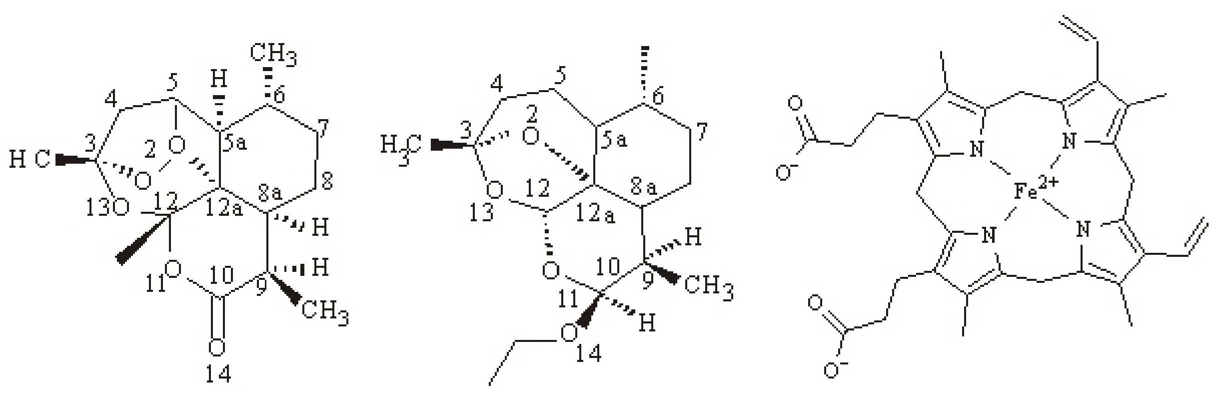

(a) (b) (c)

Fig. 1: Structures and relevant numbering system of the molecules investigated: (a) Artemisinin (QHS) (b) Deoxyartemisinin and (c) Haem

$$\text{Log(RA)} = \log[(\text{artemisinin } IC_{50}/\text{analogue } IC_{50})(\text{analogue MW}/\text{artemisinin MW})] \quad (1)$$

Molecular models of the artemisinin and its analogues (Table 1) were built using the Builder feature in Maestro (Schrodinger package) and energy was minimized in a vacuum using Impact. Each structure was assigned an appropriate bond order using ligprep script shipped by Schrödinger and optimized initially by means of the OPLS 2005 force field using default setting. Complete geometrical optimization of these structures was performed at HF/3-21G level of theory (present study) using Jaguar (Schrodinger Inc.). In order to check the reliability of the geometry obtained, we compared the structural parameters of the artemisinin 1, 2, 4-trioxane ring with theoretical (Leban *et al*., 1988) and experimental (Fersht, 1984; Lisgarten *et al*., 1998) values from the literature. All calculations reproduced most of the structural parameters of the artemisinin 1, 2, 4-trioxane ring seen in X-ray structures (Table 2). This applies especially to the bond length of the endoperoxide bridge which seems to be responsible for the anti-malarial activity.

Docking of the ligands: All the ligands were docked to the haem receptor using Glide. After ensuring that protein and ligands are in correct form for docking, the receptor-grid files were generated using grid-receptor generation program, using van der Waals scaling of the receptor at 0.4. The default size was used for the bounding and enclosing boxes. The grid box was generated at the centroid of the haem receptor. The ligands were docked initially using the "standard precision" method and further refined using "xtra precision" Glide algorithm. For the ligand docking stage, van der Waals scaling of the ligand was set at 0.5. Of the 50,000 poses that were sampled, 4,000 were taken through minimization (conjugate gradients 1,000) and the 30 structures having the lowest energy conformations were further evaluated for the favorable Glide docking score. A single best conformation for each ligand was considered for further analysis.

Rescoring using Prime/MM-GBSA: For each ligand, the pose with the lowest Glide score was rescored using Prime/MM-GBSA approach (Lyne *et al*., 2006). This approach has been used to predict the free energy of binding for set of ligands to receptor. The docked poses were minimized using the local optimization feature in Prime and the energies of complex were calculated using the OPLS-AA force field and generalized-Born surface area (GBSA) continuum solvent model. The binding free energy (G_{bind}) is then estimated using the equation:

$$G_{bind} = E_{R:L} - (E_R + E_L) + G_{solv} + G_{SA} \quad (2)$$

where $E_{R:L}$ is energy of the complex, $E_R + E_L$ is sum of the energies of the ligand and unliganded receptor, the outcome of the use of OPLS-AA force field, G_{solv} (G_{SA}) is the difference between GBSA solvation energy (surface area energy) of complex and sum of the corresponding energies for the ligand and unliganded protein. Corrections for entropic changes were not applied to this type of free energy calculation.

In order to explore the reliability of the proposed models we used the cross validation method. Prediction error sum of squares (PRESS) is a standard index to measure the accuracy of a modeling method based on the cross validation technique. The r^2_{cv} was calculated in accordance with the *PRESS* and *SSY* (sum of squares of deviations of the experimental values from their mean) using the following formula.

$$r^2_{cv} = 1 - \frac{PRESS}{SSY} = 1 - \frac{\sum_{i=1}^{n}\left(y_{exp} - y_{pred}\right)^2}{\sum_{i=1}^{n}\left(y_{exp} - \bar{y}\right)^2}$$

Where y_{exp} , y_{pred} and $\bar{y}$ are the predicted, observed and mean values of the anti-malarial activities of the artemisinin analogues.

RESULTS AND DISCUSSION

To better understand the mechanism of interaction and anti-malarial activity of artemisinin structural derivatives, computer-aided docking procedures were performed between the drug and its putative receptor. The mode of interaction of artemisinin analogues depends partly on the electrostatic configuration of the haem. Both the artemisinin (QHS) and deoxyartemisinin (DQHS) derivatives have similar structures with polar and non-polar regions. The polar regions, where the oxygen is clustered are negatively charged. QHS has two prominent negative regions (endoperoxide oxygen bridge) and both may interact with the porphyrin iron bridge. Because the DQHS derivatives lack peroxide bridge and are inactive, it was presumed that the main interaction in QHS derivatives is between the peroxide bridge and the haem-iron. Docking methods have been applied here to this study to test whether the peroxide bridge performs an important role in binding to haem. For QHS the atoms O1, O2, O13 and O11 were tested for interaction with haem-iron. Similarly for DQHS the interacting oxygen atoms; O2, O13 and O11 were tested for interaction with haem-iron. Here both the oxygen from the peroxide bridge is in close proximity to the positive iron than the other two. This indicates that the interaction between QHS and haem involves binding between the endoperoxide (O1 and O2) bridge. The respective distances of the oxygen with respect to the haem-iron are given in Table 3. The docking process was able to place QHS derivatives at distances of 3.89 (± 1.19) Å, 4.46 (± 1.13) Å, 5.61 (±0.64) Å and 5.53 (± 0.63) Å with respect

Table 3: Results for docking of haem-pdb with artemisinin (QHS) analogues as well as computed activity using Glide score as a descriptor.

Ligands	Fe-O1 distance (Å)	Fe-O2 distance (Å)	Fe-O13 distance (Å)	Fe-O11 distance (Å)	Glide score	pIC_{50expt}	$pIC_{50Gscore}$
1	2.55	3.78	5.57	5.73	-2.24	1.40	1.50
2	3.06	3.26	5.53	5.83	-1.58	0.71	0.51
3	5.20	5.37	4.09	4.85	-0.76	- 0.76	- 0.73
4	2.91	3.30	5.73	5.56	-2.21	1.19	1.46
5	3.37	4.25	6.14	5.09	-1.62	0.26	0.57
6	3.24	3.57	5.58	5.52	-1.32	0.51	0.11
7	4.17	4.72	5.75	5.93	-1.22	- 0.12	- 0.04
8	2.52	3.17	5.49	5.38	-2.27	1.60	1.55
9	5.20	5.38	6.17	5.87	-1.10	- 0.20	- 0.22
10	2.63	3.12	5.15	5.67	-1.94	1.78	1.05
11	2.64	3.65	5.64	5.43	-2.29	1.16	1.58
12	3.01	5.08	5.60	5.65	-1.18	0.26	- 0.10
13	3.34	4.56	6.61	5.80	-1.85	0.39	0.91
14	3.56	4.76	5.06	5.01	-1.21	0.34	- 0.05
15	5.41	5.42	5.13	4.96	-1.08	- 0.38	- 0.24
16	3.76	3.40	5.79	5.46	-1.56	0.67	0.48
17	2.52	3.89	6.01	5.53	-2.29	1.59	1.58
18	5.89	5.80	4.75	5.24	-0.92	- 1.44	- 0.49
19	4.85	4.92	6.49	5.20	-1.50	- 0.49	0.39
20	4.78	5.51	5.76	6.44	-1.04	- 0.02	- 0.31
21	6.63	6.32	5.82	5.13	-1.02	- 0.56	- 0.34
22	3.06	3.47	5.36	5.34	-2.21	1.34	1.46
23	3.18	3.27	5.57	5.70	-1.60	0.88	0.54
24	3.30	4.22	6.13	5.91	-1.50	0.40	0.39
25	2.83	3.37	5.52	5.10	-2.07	1.17	1.25
26	3.14	3.33	5.61	5.39	-1.72	0.94	0.72
27	3.16	3.74	5.70	5.57	-1.62	0.69	0.57
28	2.46	3.31	5.07	5.85	-2.22	1.29	1.47
29	3.90	3.91	5.45	5.44	-1.38	0.61	0.20
30	3.14	3.26	5.91	5.61	-1.77	0.87	0.79
31	3.11	3.18	5.01	5.82	-1.44	0.98	0.29
32	3.96	4.35	5.46	5.53	-1.24	- 0.40	0.01
33	3.24	5.29	6.00	5.68	-1.11	0.11	- 0.20
34	6.25	6.30	4.00	4.66	-0.46	- 0.56	- 1.19
35	3.56	3.68	5.18	5.17	-1.41	0.67	0.25
36	2.53	3.29	5.56	5.06	-2.32	1.68	1.62
37	2.71	3.14	5.00	5.38	-2.18	1.07	1.41
38	3.60	4.66	6.44	6.02	-1.54	0.28	0.45
39	3.15	3.16	5.57	5.93	-1.62	0.80	0.57
40	2.42	3.74	5.74	5.56	-2.19	1.11	1.43
41	3.56	4.42	5.74	5.70	-1.24	0.40	- 0.01
42	3.17	3.23	4.99	5.97	-1.60	0.80	0.54
43	3.38	4.53	5.71	5.41	-1.25	0.36	0.01
44	3.24	4.93	5.28	5.85	-1.11	0.22	- 0.20
45	3.95	5.16	6.40	5.83	-1.50	0.14	0.39
46	2.24	3.04	5.47	5.14	-2.11	2.07	1.30
47	2.18	2.29	5.39	5.45	-2.27	2.53	1.54
48	2.60	3.55	5.86	5.66	-2.17	1.13	1.40
49	2.44	3.06	5.24	5.31	-2.32	1.96	1.62
50	2.84	3.29	5.13	5.02	-2.11	1.02	1.31
51	2.74	3.89	5.35	5.51	-2.18	1.13	1.41
52	3.65	4.67	6.39	5.32	-1.33	0.86	0.13
53	5.58	5.78	6.05	5.81	-1.06	- 0.27	- 0.27
54	5.40	5.66	5.19	6.40	-1.07	- 0.22	- 0.27
55	5.71	6.71	5.40	5.62	-0.97	- 0.62	- 0.42
56	3.86	3.95	5.17	6.14	-1.32	0.50	0.11
57	2.52	3.19	5.14	5.35	-2.20	1.68	1.44
58	2.50	3.22	5.84	5.70	-2.19	1.22	1.43
59	5.82	5.63	5.02	6.19	-0.90	- 0.52	- 0.52
60	3.54	4.41	5.39	5.99	-1.28	0.44	0.05
61	3.54	3.41	5.76	5.69	-1.65	0.61	0.61
62	4.04	5.81	7.35	6.75	-1.55	- 0.11	0.46
63	3.89	4.53	5.55	6.10	-1.20	0.28	- 0.07
64	3.14	4.00	6.17	5.38	-1.38	0.93	0.20
65	4.77	5.50	5.67	5.12	-1.08	0.00	- 0.25
66	2.58	3.26	5.57	5.58	-2.13	1.04	1.34
67	3.47	3.58	5.54	6.38	-1.31	0.73	0.10
68	4.74	4.02	6.20	5.14	-1.24	- 0.32	- 0.02
69	3.68	4.72	6.39	5.97	-1.56	0.46	0.48

Table 3: (Continued)

Ligands	Fe-O1 distance (Å)	Fe-O2 distance (Å)	Fe-O13 distance (Å)	Fe-O11 distance (Å)	Glide score	pIC_{50expt}	$pIC_{50Gscore}$
70	5.530	6.52	4.430	4.920	-0.68	- 0.59	- 0.85
71	3.360	4.52	5.430	6.410	-1.24	0.40	- 0.01
72	5.790	6.02	4.410	4.650	-0.72	- 0.45	- 0.79
73	3.450	4.41	6.140	6.420	-1.62	0.17	0.57
74	5.700	6.51	5.100	4.740	-0.76	- 0.65	- 0.73
75	5.790	6.34	4.770	4.480	-0.62	- 1.43	- 0.94
76	3.990	4.03	6.110	6.760	-1.53	0.60	0.43
77	6.240	6.86	4.170	5.070	-0.56	- 1.45	- 1.03
78	6.040	7.22	4.010	4.880	-0.33	- 1.56	- 1.38
79	3.650	4.57	5.740	6.060	-1.29	0.43	0.07
80	2.720	3.11	5.270	5.540	-2.29	1.20	1.58
81	5.270	5.46	5.160	4.980	-1.01	- 0.80	- 0.35
82	4.470	4.02	5.950	4.800	-1.27	- 0.37	0.04
83	5.450	6.08	5.220	5.710	-1.14	- 0.20	0.45
84	6.160	6.14	5.450	5.650	-0.54	- 1.76	- 1.06
85	5.160	6.15	4.210	4.800	-0.51	- 2.09	- 1.11
86	4.750	6.08	6.840	7.280	-1.54	- 0.36	0.45
87	3.430	4.19	5.940	5.730	-1.54	0.49	- 0.27
88	4.720	4.53	5.390	6.040	-1.15	- 0.18	- 0.15
89	6.440	5.03	6.240	5.380	-0.94	- 0.83	- 0.46
90	3.860	4.92	5.610	5.710	-1.23	0.40	- 0.02
91	5.380	5.59	4.630	4.990	-1.07	- 0.37	0.57
92	3.490	4.48	6.250	5.550	-1.62	0.18	- 0.95
93	5.520	5.91	4.940	5.320	-0.62	- 1.90	- 0.40
94	5.460	5.68	5.530	4.680	-0.98	- 1.28	- 0.35
95	4.030	5.36	5.600	5.880	-1.01	- 0.11	0.64
96	3.710	4.75	6.480	6.490	-1.67	- 0.06	- 0.20
97	3.340	5.35	6.050	5.910	-1.11	0.01	- 0.20
98	3.170	3.19	5.340	6.860	-1.54	0.91	0.45
99	2.210	2.46	5.610	5.380	-2.38	2.37	1.71
100	3.170	3.18	4.100	5.460	-1.48	0.86	0.35
101	3.340	4.87	6.130	6.310	-1.45	0.22	0.31
102	5.720	5.48	3.730	4.730	-0.64	- 0.38	- 0.91
103	4.910	5.33	6.510	6.970	-1.59	- 0.33	0.52
104	3.830	5.53	6.410	6.250	-1.48	- 0.10	0.35
105	3.050	5.40	5.580	5.780	-1.12	0.13	- 0.19
106	3.590	4.84	6.130	5.210	-1.25	0.40	0.01
107	2.880	3.08	5.490	5.960	-2.25	1.79	1.52
108	5.620	3.96	5.890	6.940	-1.58	- 0.18	0.51
109	5.970	6.48	4.510	3.060	-0.46	- 0.28	- 1.19
110	2.810	3.68	5.160	5.360	-2.13	1.24	1.34
111	5.930	6.03	6.480	5.060	-1.13	- 0.25	- 0.18
112	2.410	3.22	5.650	5.610	-2.21	1.24	1.46
113	2.490	3.06	5.640	5.130	-2.23	1.24	1.49
114	2.960	3.49	5.770	5.170	-2.24	1.24	1.50
115	3.140	3.50	4.570	5.020	-1.50	0.85	0.39
116	2.440	3.19	5.440	5.300	-2.16	1.07	1.38
117	2.670	3.63	5.770	5.770	-2.22	1.24	1.47
118	3.860	3.66	5.080	6.470	-1.65	0.64	0.61
119	3.940	3.80	5.970	5.800	-1.62	0.50	0.57
120	3.630	4.28	5.540	5.870	-1.26	0.45	0.02
121	2.270	3.18	5.470	5.740	-2.18	1.20	1.41
122	3.390	4.62	5.840	6.910	-1.72	0.01	0.72
123	3.170	3.62	5.000	6.380	-1.23	0.66	- 0.02
124	5.960	6.01	4.930	4.150	-0.76	- 1.71	- 0.73
125	3.660	4.62	5.510	6.360	-1.23	0.34	- 0.02
126	3.810	3.45	5.820	7.160	-1.69	0.71	0.67
127	3.160	3.19	5.320	6.420	-1.54	0.73	0.45
128	5.240	6.53	6.140	5.870	-0.93	- 0.20	- 0.48
129	6.670	6.11	3.910	3.990	-0.35	- 1.77	- 1.35
130	4.060	4.84	6.640	6.530	-1.58	- 0.09	0.51
131	4.130	4.76	5.900	6.560	-1.48	- 0.12	0.35
132	2.590	3.73	5.590	5.140	-1.92	1.59	1.02
133	5.479		4.327	5.435	-3.61	- 3.62	- 3.63
134	4.141		5.778	4.916	-3.56	- 3.63	- 3.64
135	4.295		5.893	5.995	-3.52	- 3.68	- 3.65
136	4.697		6.831	6.378	-3.75	- 3.60	- 3.59
137	4.297		5.211	5.539	-3.49	- 3.66	- 3.66
138	3.934		6.186	5.892	-3.60	- 3.62	- 3.63

Table 3: (Continued)

Ligands	Fe-O1 distance (Å)	Fe-O2 distance (Å)	Fe-O13 distance (Å)	Fe-O11 distance (Å)	Glide score	pIC_{50expt}	$pIC_{50Gscore}$
139	3.957		6.147	6.604	-3.51	-3.67	-3.65
140	5.118		3.296	4.587	-3.43	-3.66	-3.68
141	5.271		4.438	4.860	-3.59	-3.61	-3.63
142	4.005		5.671	4.578	-3.54	-3.66	-3.65
143	5.404		4.077	4.341	-3.58	-3.65	-3.64
144	4.413		6.282	5.339	-3.70	-3.59	-3.60

Table 4: Results for rescoring using Prime/MM-GBSA of haem-pdb with artemisinin analogues as well as computed activity using ΔG_{bind} energy as a descriptor.

Ligands	Fe-O1 distance(Å)	Fe-O2 distance(Å)	Fe-O13 distance(Å)	Fe-O11 distance(Å)	ΔG_{bind} kcal/mol	pIC_{50expt}	$pIC_{50\Delta Gbind}$
1	2.580	2.661	4.407	5.842	-6.68	1.40	0.79
2	3.148	3.528	5.659	4.803	-6.55	0.71	0.68
3	3.006	2.688	5.044	4.761	-5.12	- 0.65	- 0.57
4	2.363	3.370	5.070	5.712	-6.63	1.19	0.75
5	3.097	3.247	5.408	4.588	-6.09	0.28	0.28
6	3.087	3.209	5.391	4.617	-6.11	0.51	0.30
7	3.286	3.795	5.758	4.704	-5.35	- 0.12	- 0.36
8	3.390	3.266	5.116	5.558	-6.76	1.60	0.86
9	3.162	4.943	5.586	6.330	-4.13	- 2.09	- 1.43
10	2.880	3.340	5.134	5.693	-7.12	1.78	1.18
11	2.956	3.245	5.500	5.429	-6.46	1.16	0.60
12	3.059	3.353	5.603	5.662	-6.49	0.26	0.63
13	4.301	4.582	5.765	4.989	-6.26	0.39	0.43
14	3.522	3.852	5.073	4.811	-6.21	0.34	0.39
15	3.150	3.909	6.150	3.740	-4.95	- 0.38	- 0.71
16	3.723	3.207	4.542	5.243	-6.36	0.67	0.52
17	2.995	2.898	5.117	5.580	-6.76	1.59	0.86
18	3.504	5.126	6.143	6.148	-4.53	- 1.43	- 1.08
19	3.518	4.453	6.101	4.808	-5.85	- 0.45	0.07
20	4.110	4.836	5.241	5.891	-6.58	- 0.02	0.71
21	4.890	5.264	5.588	4.913	-5.86	- 0.52	0.08
22	2.558	3.396	5.190	4.874	-6.30	1.34	0.46
23	3.146	3.740	5.019	5.917	-6.92	0.88	1.00
24	2.872	2.660	4.997	4.952	-6.24	0.40	0.41
25	2.810	3.049	5.288	4.923	-6.36	1.17	0.52
26	3.284	3.412	5.704	5.624	-7.01	0.94	1.08
27	3.725	3.575	4.902	5.850	-7.17	0.69	1.22
28	2.594	3.261	4.661	5.408	-6.40	1.29	0.55
29	3.030	3.133	5.567	5.560	-7.08	0.61	1.14
30	3.295	3.211	4.867	4.625	-5.95	0.87	0.16
31	4.818	5.461	6.130	6.668	-6.97	0.98	1.05
32	3.691	3.883	4.011	5.455	-6.06	0.40	0.25
33	3.452	4.330	4.013	5.210	-5.12	0.11	- 0.57
34	3.940	4.796	6.426	6.296	-4.84	- 0.56	- 0.81
35	3.773	3.821	4.896	5.473	-7.16	0.67	1.21
36	3.367	3.492	5.689	4.973	-7.18	1.68	1.23
37	3.273	3.336	5.650	5.509	-7.00	1.07	1.07
38	3.174	3.024	5.129	4.351	-5.67	0.28	- 0.09
39	3.034	3.159	5.909	5.262	-7.26	0.80	1.30
40	2.830	3.580	4.859	5.797	-6.97	1.11	1.05
41	3.718	3.801	4.941	5.479	-6.28	0.40	0.45
42	3.806	3.576	4.817	5.754	-7.22	0.80	1.27
43	4.158	4.716	4.897	5.537	-6.23	0.36	0.40
44	3.357	3.985	5.245	5.784	-6.04	0.22	0.24
45	4.088	4.349	4.550	6.002	-6.20	0.14	0.38
46	2.180	3.052	5.780	5.980	-7.60	2.07	1.60
47	2.392	2.420	5.390	6.390	-7.85	2.53	1.82
48	2.834	3.710	4.009	5.899	-6.09	1.13	0.28
49	2.775	2.785	5.120	6.140	-7.45	1.96	1.47
50	2.722	3.813	5.462	4.933	-6.44	1.02	0.59
51	2.496	3.421	5.079	4.955	-6.20	1.13	0.38
52	3.703	4.673	5.522	5.667	-7.21	0.86	1.26
53	4.572	4.858	5.045	5.669	-6.13	- 0.25	0.32
54	4.299	4.582	5.901	3.834	-5.27	- 0.20	- 0.43
55	3.517	4.981	5.740	6.557	-4.58	- 0.59	- 1.04
56	2.902	2.882	5.110	6.138	-6.63	0.50	0.75

Table 4: (Continued)

Ligands	Fe-O1 distance(Å)	Fe-O2 distance(Å)	Fe-O13 distance(Å)	Fe-O11 distance(Å)	ΔG_{bind} kcal/mol	pIC_{50expt}	$pIC_{50\Delta Gbind}$
57	2.086	3.194	5.930	5.140	-7.01	1.68	1.08
58	2.739	3.448	5.079	6.094	-7.36	1.22	1.39
59	4.617	4.629	5.788	4.018	-5.07	- 0.49	- 0.61
60	3.803	3.733	5.620	5.222	-6.72	0.44	0.83
61	3.726	3.662	4.062	5.946	-6.49	0.61	0.63
62	4.489	5.670	5.332	5.625	-6.36	- 0.11	0.52
63	3.963	3.530	4.542	5.278	-6.07	0.26	0.26
64	3.274	3.994	4.403	6.193	-7.13	0.93	1.19
65	4.881	5.185	5.238	5.299	-6.11	0.00	0.30
66	2.699	3.431	4.185	6.030	-6.55	1.04	0.68
67	2.852	3.440	5.565	5.449	-7.25	0.73	1.29
68	4.866	4.241	4.305	5.342	-5.58	- 0.28	- 0.16
69	3.794	4.878	5.535	5.219	-6.94	0.46	1.02
70	3.010	2.936	5.272	5.588	-6.09	- 0.56	0.28
71	4.011	4.205	4.527	5.759	-6.48	0.40	0.62
72	4.327	4.943	5.967	6.246	-5.02	- 0.38	- 0.65
74	3.576	4.326	5.128	4.885	-4.96	- 0.62	- 0.70
75	3.523	3.477	4.646	5.155	-5.04	- 1.28	- 0.64
76	3.582	3.572	5.285	5.328	-7.05	0.60	1.12
77	3.606	4.604	5.319	3.670	-4.48	- 1.44	- 1.12
78	4.943	4.069	5.133	3.190	-4.30	- 1.45	- 1.28
79	3.746	4.042	5.356	5.943	-6.91	0.43	1.00
80	3.062	3.641	5.069	6.113	-7.24	1.20	1.28
81	3.223	3.194	5.387	4.590	-5.76	- 0.76	- 0.01
82	3.413	3.887	5.830	4.755	-5.65	- 0.37	- 0.10
83	4.152	4.245	5.279	4.654	-5.37	- 0.20	- 0.35
84	3.951	4.445	5.710	6.066	-4.83	- 0.98	- 0.82
86	3.967	4.579	5.864	4.964	-5.96	- 0.33	0.17
87	3.601	3.757	4.153	5.790	-6.25	0.49	0.42
88	3.682	4.339	4.828	4.627	-5.29	- 0.18	- 0.42
89	4.398	5.610	5.773	4.450	-5.70	- 0.80	- 0.06
90	2.890	3.901	5.603	5.766	-6.38	0.40	0.53
91	4.528	4.871	4.032	5.267	-4.86	- 0.36	- 0.79
92	3.390	3.463	5.198	5.721	-6.27	0.18	0.44
93	3.077	3.557	5.557	3.340	-4.29	- 1.77	- 1.29
94	3.846	5.050	5.629	5.905	-4.72	- 0.83	- 0.91
95	4.610	4.738	4.582	4.782	-5.35	- 0.11	- 0.36
96	4.170	4.732	5.085	6.051	-6.58	- 0.06	0.71
97	3.486	4.449	5.128	6.038	-6.46	0.01	0.60
98	3.674	3.685	5.177	5.883	-7.39	0.91	1.41
99	2.750	2.550	5.570	6.100	-7.88	2.37	1.84
100	3.123	3.109	4.283	4.825	-5.59	0.86	- 0.16
101	4.059	4.434	6.065	3.800	-5.53	0.22	- 0.21
102	3.910	4.549	4.828	5.129	-5.01	- 0.37	- 0.66
103	4.022	4.404	5.293	5.636	-6.14	- 0.32	0.32
104	4.092	4.555	4.168	5.663	-5.40	- 0.10	- 0.32
105	3.230	3.535	5.667	5.031	-6.09	0.13	0.28
106	3.969	3.862	5.791	5.095	-6.66	0.40	0.78
107	2.703	3.227	5.427	6.080	-7.27	1.79	1.31
108	4.051	4.253	5.274	3.736	-5.00	- 0.18	- 0.67
109	4.210	4.819	4.926	4.415	-5.11	- 0.27	- 0.57
110	2.917	3.704	4.822	5.480	-6.40	1.24	0.55
111	3.964	4.391	4.332	5.174	-5.18	- 0.22	- 0.51
112	2.940	2.859	4.189	5.357	-5.85	0.87	0.07
113	2.774	3.770	4.963	5.487	-6.28	1.24	0.45
114	2.978	3.070	4.537	5.122	-6.27	1.24	0.44
115	3.152	3.676	4.696	5.079	-5.97	0.85	0.18
116	2.886	3.662	4.991	5.326	-6.45	1.07	0.59
117	2.958	2.977	5.719	4.227	-6.40	1.24	0.55
118	3.961	3.814	5.241	5.525	-7.07	0.64	1.14
119	3.230	2.615	4.744	5.844	-7.03	0.50	1.10
120	3.961	3.588	5.489	5.021	-6.86	0.45	0.95
121	2.540	3.273	5.504	5.936	-7.20	1.20	1.25
122	3.420	4.370	5.420	5.372	-6.06	0.01	0.25
123	3.228	2.735	5.118	5.445	-6.46	0.66	0.60
124	3.561	4.208	5.891	5.682	-4.15	- 1.56	- 1.41
125	3.631	3.604	5.417	5.253	-6.11	0.34	0.30
126	3.990	4.348	5.306	5.437	-6.87	0.71	0.96
127	3.141	3.251	5.605	5.609	-7.23	0.73	1.27

Table 4: (Continued)

Ligands	Fe-O1 distance(Å)	Fe-O2 distance(Å)	Fe-O13 distance(Å)	Fe-O11 distance(Å)	ΔG_{bind} kcal/mol	pIC_{50expt}	$pIC_{50\Delta Gbind}$
128	3.644	3.200	5.387	4.956	-5.80	- 0.20	0.03
129	4.117	4.361	6.79	6.095	-4.76	- 1.76	- 0.88
130	4.241	5.023	4.847	5.733	-5.82	- 0.09	0.05
131	3.516	3.727	5.902	5.005	-6.06	- 0.12	0.25
132	2.702	2.775	5.128	5.340	-6.98	1.59	1.06
133	5.622		4.364	5.548	-8.51	- 3.62	- 3.63
134	4.451		6.029	4.969	-8.29	- 3.63	- 3.63
135	3.806		5.92	6.099	-4.85	- 3.68	- 3.69
136	4.811		6.963	6.441	-9.80	- 3.60	- 3.61
137	4.420		6.613	6.774	-8.13	- 3.66	- 3.64
138	4.274		6.521	6.215	-8.35	- 3.62	- 3.63
139	4.845		6.935	7.543	-7.16	- 3.67	- 3.65
140	5.263		3.580	4.761	-6.49	- 3.66	- 3.67
141	5.807		5.500	5.706	-9.73	- 3.61	- 3.61
142	4.378		5.747	4.565	-8.02	- 3.66	- 3.64
143	5.693		4.293	4.488	-8.45	- 3.65	- 3.63
144	4.565		5.947	4.712	-10.01	- 3.59	- 3.60

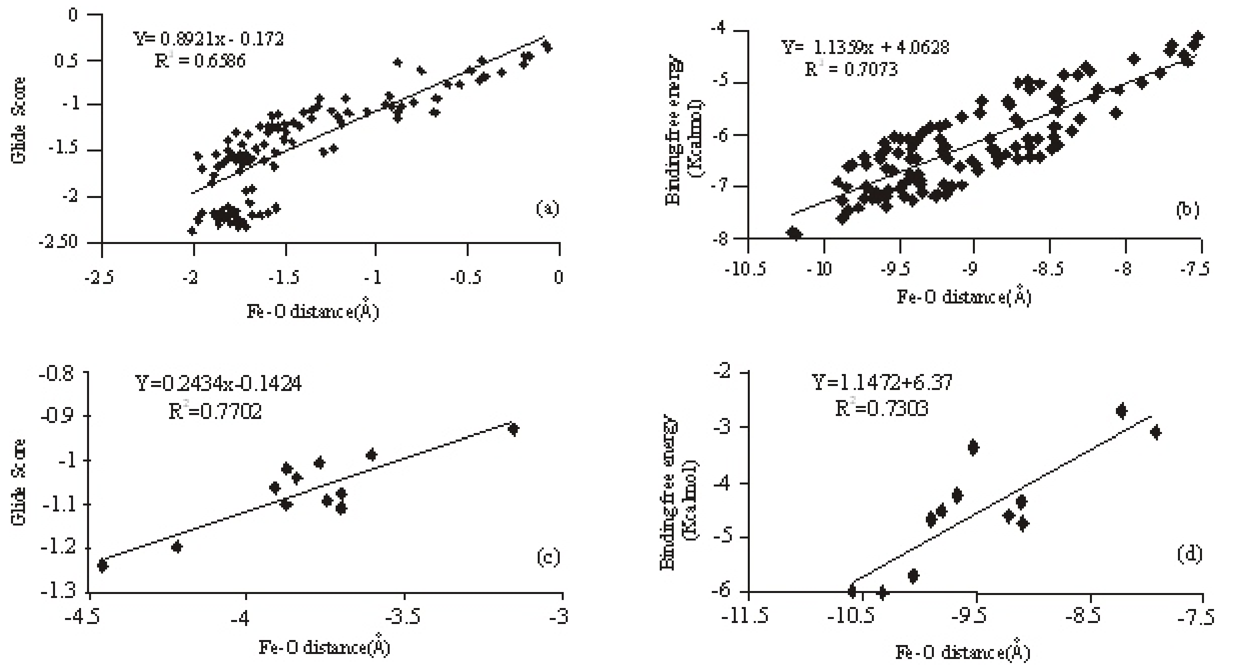

Fig. 2(a-d): A linear relationship between Fe-O distance and Glide score as well as Fe-O distance and binding free energy of the (a and b) Artemisinin (QHS) derivatives and (c and d) Deoxyartemisinin (DQHS) derivatives. The Fe-O distance represents the optimized value of the distances obtained by linear combination of distances between O1-Fe, O2-Fe, O13-Fe and O11-Fe atom pairs respectively between QHS analogues and haem-iron: O-Fe distance = α (O1-Fe) + β (O2-Fe) + γ (O13-Fe) + δ (O11-Fe). The α, β, γ and δ are fitting parameters. The values obtained for the four fitting parameters, α, β, γ and δ are 0.101, 0.191, -0.357, -0.129 and -0.482, 0.798, -0.520, -0.905 respectively using Glide score and binding free energy as dependent variables. The optimized equation obtained for O-Fe distance for deoxyartemisinin derivatives was: O-Fe distance = α (O2-Fe) + β (O13-Fe) + γ (O11-Fe). The values obtained for the three fitting parameters α, β and γ are -0.431, -0.490, 0.144 and -1.43, -1.18, 0.74 respectively using Glide score and binding free energy as dependent variables

to O1, O2, O13 and O11 oxygen atoms respectively from haem-iron. DQHS derivatives have single oxygen instead of the peroxide bridge. The haem-iron could interact with DQHS in several ways. Form the docking result it has been seen that the haem-iron preferentially interact either at the side involving all the three non-peroxide oxygen O2, O13 and O14 or the peroxide derived oxygen O11. Thus, the active anti-malarial QHS clearly interacts with haem in a manner different from its inactive analogue DQHS. Haem catalyzes the breakdown of artemisinin (Zhang *et al.*, 1992) into a free radical (Meshnick *et al.*, 1993) and/or electrophilic intermediate (Posner and Oh, 1992). Once formed, this intermediate can alkylate haem (Hong *et al.*, 1994) or protein (Yang *et al.*, 1993). The orientation of QHS with respect to haem may be critical to the formation of this intermediate and thus for drug action. Thus molecular docking and rescoring using Prime/MM-GBSA may aid in the design of new QHS congeners.

We applied the docking MM-GB/SA method to a data set of 144 artemisinin analogues to build a binding affinity model for evaluating anti-malarial activity. The data set used for building the binding affinity model comprised nine subsets of artemisinin analogues (Table 1). These compounds were taken from various sources, among these are endoperoxide artemisinin analogues, 10-substituted artemisinin derivatives, artemisinin derivatives without D-ring, 9-substituted artemisinin derivatives, dihydroartemisinin derivatives, tricyclic 1, 2, 4-trioxanes, 3C-substituted artemisinin derivatives, deoxyartemisinin analogues and miscellaneous artemisinin derivatives. The experimental relative activity (RA) values for all those compounds were calculated against the drug resistant malarial strain *P. falciparum* (W-2 clone). The IC_{50} value of these analogues was derived from the equation 1 and used for calculation of absolute pIC_{50} (pIC_{50} = - log IC_{50}). With the wide range of difference in pIC_{50} values and the large diversity in the structures, the combined set of 144 ligands is ideal to build the affinity binding model as the set does not suffer from bias due to the similarity of the structures. This data set compounds were docked into the haem receptor site using the Glide-XP module and rescore using Prime/MM-GBSA (Schrodinger, Inc.). For the better understanding of the mechanism of action of the artemisinin analogues all the 144 compounds were classified into highly potent, low and inactive analogues based on the experimental pIC_{50}.

All the active artemisinin (QHS) derivatives (1-132, Table 1) were found to be good binder with haem (Table 3). We can observe that the most potent artemisinin analogues (pIC_{50} > 1.0) were found to have better docking score in comparison to the analogues which are less potent (pIC_{50} < 1.0). For the highly potent analogues the distances between O1-Fe, O2-Fe, O13-Fe and O11-Fe atom pairs were 2.59 (± 0.22) Å, 3.31 (± 0.36) Å, 5.49 (± 0.25) Å and 5.45 (± 0.24) Å respectively; the glide score obtained was -2.20 (± 0.11). However, for the less potent analogues the distances were found to be 4.31 (± 1.08) Å, 4.83 (± 1.03) Å, 5.54 (± 0.71) Å and 5.67 (± 0.71) Å respectively for the O1-Fe, O2-Fe, O13-Fe and O11-Fe atom pairs; the glide score was -1.24 (± 0.36) (Table 3). A linear relationship between Glide score and optimized O-Fe distance was obtained with R^2 value of 0.6586 (Fig. 2a). The optimized O-Fe distance was obtained by linear combination of O1-Fe, O2-Fe, O13-Fe and O11-Fe atom pairs between the oxygen of artemisinin and haem-iron as explained in Fig. 2. It has been seen that the distances between O1-Fe and O2-Fe are more important for the activity of artemisinin analogues. For the inactive artemisinin (DQHS) analogues (pIC_{50} < -3.0) which lack the peroxide bridge the Glide score was found to be -1.07 (± 0.09) (Table 3). The distances for O2-Fe, O13-Fe and O11-Fe atom pairs were 4.58 (± 0.59) Å, 5.34 (± 1.08) Å and 5.37 (± 0.74) Å respectively. Further, a linear relationship with R^2 value of 0.7702 was obtained between Glide score and the optimized O-Fe distance (Fig. 2c). The interaction of the artemisinin with haem is very much dependent upon the stereochemistry of artemisinin analogues, a mechanism that is controlled by steric hindrance. The analogues which approach the haem-iron as close as possible will have better interaction and thus the good glide score. However, owing to the planar structure of the haem-model, the repulsion between artemisinin and the protoporphyrin ring of haem prevents artemisinin from approaching haem-iron.

For each ligand in the virtual library, the pose with the lowest Glide score was rescored using Prime/MM-GBSA approach. Rescoring using Prime/MM-GBSA leads to minor changes of the ligand conformations within receptor site. These changes result from minimization of the ligand in receptor's environment and consequent stabilization of receptor:ligand complex. This approach is used to predict the binding free energy (G_{bind}) for set of ligands to receptor. Table 4 reveals the G_{bind} energy of artemisinin analogues. The G_{bind} energy of the highly potent QHS analogues (pIC_{50} > 1.0) were higher (-6.84 ± 0.50 kcal/mol) than less potent analogues (-5.96 ± 0.84 kcal/mol) and inactive DQHS derivatives (-4.47 ± 1.07 kcal/mol). The distances between O1-Fe, O2-Fe, O13-Fe and O11-Fe atom pairs for most potent analogues were 2.77 (± 0.30) Å, 3.23 (± 0.35) Å, 5.13 (± 0.46) Å and 5.57 (± 0.49) Å respectively. The binding affinity of the artemisinin derivatives with haem is very much dependent upon the proximity of O1 and O2 atoms. On the contrary, for the less potent analogues the distances were 3.69 (± 0.53) Å, 4.03 (± 0.71) Å, 5.25 (± 0.57) Å and 5.26 (± 0.71) Å. For the inactive DQHS derivatives the distances for O2-Fe, O13-Fe and O11-Fe atom pairs were 4.83 (± 0.64) Å, 5.70 (± 1.09) Å and 5.65 (± 0.98) Å respectively. A linear relationship between linear combination of O-Fe distances and G_{bind} energy was obtained (Fig. 2b & 2d) with R^2 value of 0.7073 and 0.7303 for the QHS and DQHS derivatives respectively.

Building models for prediction of pIC_{50} using Glide score and binding free energy: A prediction model of anti-malarial activity (pIC_{50}) was built based on Glide score and G_{bind} as descriptors. The plot of the Glide score and experimental pIC_{50} reveal a significant relationship (R^2 = 0.763 and R^2 = 0.734 for both the QHS and DQHS derivatives) between these two parameters (Fig. 3a & 3c). A linear regression model for prediction of predicted pIC_{50} of anti-malarial activity based on Glide score has been developed by considering analogues with known pIC_{50}. The Eq. 3 and 4 of the model and the corresponding statistics for QHS & DQHS are shown below:

$$pIC_{50} = -1.88\ (\pm 0.115) - 1.51\ (\pm 0.074)^{*}\ \text{G-score} \quad (3)$$
$$(N = 132,\ r^2 = 0.763,\ r^2_{cv} = 0.762,\ s = 0.428,\ F = 419.66)$$

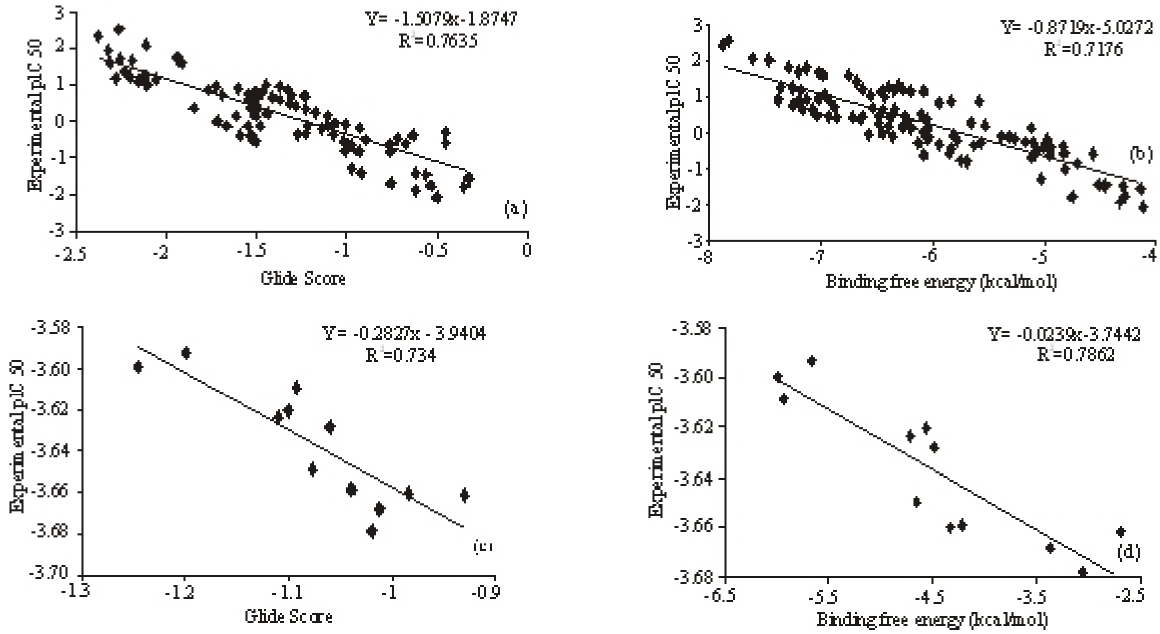

Fig. 3(a-d): Models for predicting antimalarial activity (pIC_{50}) of the (a&b)Artemisinin (QHS) analogues and (c&d) Deoxy-artemisinin analogues based on Glide score and Binding free energy (G_{bind}) as descriptor

$$pIC_{50} = -3.94 (\pm 0.061) - 0.284 (\pm 0.057)* \text{G-score} \quad (4)$$
$(N = 12, r^2 = 0.734, r^2_{cv} = 0.685, s = 0.017, F = 24.92)$

Reasonably good agreement between predicted and experimental pIC_{50} are found (root mean square error = 0.36 and 0.01 for QHS and DQHS derivatives) and suggested that the calculated pIC_{50} based on Glide score is robust and accurate. Similar prediction model of predicted pIC_{50} of anti-malarial activity has been developed by considering G_{bind} energy as a descriptor. The Eq. 5 and 6 of the model and the corresponding statistics for QHS and DQHS analogues are shown below:

$$pIC_{50} = -5.03 (\pm 0.298) - 0.872 (\pm 0.048)* G_{bind} \quad (5)$$
$(N = 132, r^2 = 0.718, r^2_{cv} = 0.715, s = 0.471, F = 330.22)$

$$pIC_{50} = -3.75 (\pm 0.019) - 0.024 (\pm 0.004)* G_{bind} \quad (6)$$
$(N = 12, r^2 = 0.786, r^2_{cv} = 0.739, s = 0.015, F = 32.20)$

The G_{bind} energy value among the ligands of QHS library varies in between -7.88 and -4.13 kcal/mol and the overall mean is -6.16 (± 0.859) kcal/mol. It revealed that all these ligands bind to haem-iron with high affinity and showed activity (experimental pIC_{50}) in between -2.09 and 2.53. On the contrary, for the DQHS derivatives the G_{bind} energy value varies between -5.66 and -2.69 kcal/mol; the experimental pIC_{50} was -3.59 to -3.66. Correspondingly, the plot of the binding free energy and experimental pIC_{50} reveals a significant relationship (R^2 = 0.718 and R^2 = 0.786 for QHS and DQHS respectively) between these two parameters (Fig. 3b & 3d). The calculated pIC_{50} based on G_{bind} energy descriptor was in good agreement with experimental pIC_{50} (root mean square error = 0.40 and 0.01 for QHS and DQHS derivatives) and suggested that the prediction model is robust and accurate.

CONCLUSION

We have compiled a virtual library of artemisinin analogues which are built through structural modification of scaffold structure of natural artemisinin. Docking and rescoring using PRIME/MM-GBSA have been used in the study to get insights into artemisinin: haem interactions and development of prediction model for anti-malarial activity. The docking result revealed that the haem-iron approaches the endoperoxide moiety at the O1 position in preference to the O2 position. Several sets of artemisinin analogues have been studied in the docking simulations. Results showed that these analogues bind in a very similar mode. The magnitude of the binding affinity can be a key factor that decides the activeness of an individual inhibitor. An energetic evaluation of the binding affinity will provide a way to estimate the activity of inhibitors. In any binding energy calculation, the correct binding structure of each ligand has to be determined first prior to the binding energy estimation. Very similar binding structures were obtained for a set of analogues. This makes a credible prediction model of the anti-malarial activity (pIC_{50}) calculation possible. The calculated Glide score and binding free energy value of a set of structural analogues demonstrate excellent linear correlation to the experimental anti-malarial activity. Thus, these models could be useful to predict the range of activity for new artemisinin analogues. We also found that refinement of poses and consequent rescoring using PRIME/MM-GBSA leads to better predictivity of pIC_{50}. The information that we have expressed in this study may lead to design (synthesis) of more potent artemisinin derivatives for inhibition of haem polymerization.

REFERENCES

Acton, N., J.M. Karle and R.E. Miller, 1993. Synthesis and antimalarial activity of some 9-substituted artemisinin derivatives. J. Med. Chem., 36: 2552-2557.

Avery, M.A., J.D. Bonk, W.K.M. Chong, S. Mehrotra and R. Miller, 1995. Structure-activity relationships of the antimalarial agent artemisinin. 2 effect of heteroatom substitution at o-11: synthesis and bioassay of N-Alkyl-11-aza-9-desmethylartemisinins. J. Med. Chem., 38: 5038-5044.

Avery, M.A., S. Mehrotra, J.D. Bonk, J.A. Vroman and D. K. Goins, 1996. Structure-activity relationships of the antimalarial agent artemisinin. 4 effect of substitution at C-3. J. Med. Chem., 39: 2900-2906.

China Cooperative Research Group 1982. On qinghaosu and its derivatives as antimalarials. J. Trad. Chin. Med., 2: 3-8.

Cumming, J.N., P. Ploypradith and G.H. Posner, 1997. Antimalarial activity of artemisinin (quinghaosu) and related trioxanes: mechanism(s) of action. Adv. Pharmacol., 37: 253-297.

Doman, T.N., S.L. McGovern, B.J. Witherbee, T.P. Kastern, R. Kurumbail, W.C. Stallings, D.T. Connolly and B.K. Shoichet, 2002. Molecular docking and high-throughput screening for novel inhibitors of protein tyrosine phosphatase-1B. J. Med. Chem., 45: 2213-2221.

Fersht, A.R., 1984. Basis of biological specificity. Trends Biochem. Sci., 9: 145-153.

Friedman, S.H., P.S. Ganapathi, , Y. Rubin and G.L. Kenyon, 1998. Optimizing the binding of fullerene inhibitors of the HIV-1Protease through predicted increases in hydrophobic desolvation. J. Med. Chem., 41: 2424-2429.

Goldberg, D.E., A.F. Slater, A. Cerami and G.B. Henderson, 1990. Hemoglobin degradation in the malaria parasite Plasmodium falciparum: An ordered process in a unique organelle. Proc. Natl. Acad. Sci. U.S.A., 87(8): 2931–2935.

Gruneberg, S., M.T. Stubbs and G. Klebe, 2002. Successful virtual screening for novel inhibitors of human carbonic anhydrase: Strategy and experimental confirmation. J. Med. Chem., 45: 3588-3602.

Gschwend, D.A., W. Sirawaraporn, D.V. Santi and I.D. Kuntz, 1997. Specificity in structure-based design: identification of novel selective inhibibtor of *Pneumocystis carinii* dihydrofolate reductas. Proteins., 29:59-67.

Hay, P.J. and W.R. Wadt, 1985. Ab initio effective core potentials for molecular calculations potentials for K to Au including the outermost core orbitals. J. Chem. Phys., 82: 299-310.

Haynes, R. K. and S. C. Vonwiller, 1996. The behaviour of qinghaosu (artemisinin) in the presence of heme iron (II) and (III). Tetrahedron. Lett., 37: 253-256.

Hong, Y.L., Y.Z.Yang and S.R. Meshnick, 1994. The interaction of artemisinin with malarial hemozoin. Mol. Biochem. Parasitol., 63: 121-128.

Jaguar, version 4.1: Schrodinger, 2000. Inc.: Portland.

Jefford, C.W., M.G.H. Vicente, Y. Jacquier, F. Favarger, J. Mareda, P. Millasson-Schmidt, G. Brunner and U. Burger, 1996. The deoxygenation and isomerization of artemisinin and artemether and their relevance to antimalarial action. Helv. Chim. Acta., 79: 1475-1487.

Jung, M., 1994. Current developments in the chemistry of artemisinin and related compounds. Curr. Med. Chem., 1: 35-42.

Klayman, D.L., 1985. Qinghaosu (artemisinin): an antimalarial drug from China. Science, 228: 1049-1055.

Leban, I., L. Golic and M. Japeli, 1988. Crystal and molecular structure of qinghaosu: a redetermination. Acta. Pharm. Jugosl., 38: 71-77.

Lin, A.J., M. Lee and K.L. Daniel, 1989. Antimalarial activity of new water-soluble dihydroartemisinin derivatives. 2 stereospecificity of the ether side chain. J. Med. Chem., 32: 1249-1252.

Lisgarten, J.N., B.S. Potter, C. Bantuzeko and R.A. Palmer, 1998. Structure, Absolute configuration, and conformation of the antimalarial compound, artemisinin. J. Chem. Cryst., 28: 539-543.

Lyne, P.D., M.L. Lamb and J.C. Saeh, 2006. Accurate prediction of the relative potencies of members of a series of kinase inhibitors using molecular docking and MM-GBSA scoring. J. Med. Chem., 49: 4805-4808.

Massova, I., P. Martin, A. Bulycheve, R. Kocz, M. Doyle, B.F.P. Edvards and S. Mobasher, 1998. Templates for design of inhibitors for serine proteases: application of the program dock to the discovery of novel inhibitors for thrombin. Bioorg. Med. Chem. Lett., 18: 2463-2466.

Meshnick, S.R., A. Thomas, A. Ranz, C.M. Xu and H.Z. Pan, 1991. Artemisinin (qinghaosu): The role of intracellular hemin in its mechanism of antimalarial action. Mol. Biochem. Parasitol., 49(2): 181-189.

Meshnick, S.R., Y.Z. Yang, V. Lima, F. Kuypers, S. Kamchonwongpaisan and Y. Yuthavong, 1993. Iron-dependent free radical generation from the antimalarial agent artemisinin (qinghaosu). Antimicrob. Agents. Chemother., 37: 1108-1117.

Pinheiro, J.C., M.M.C. Ferreira and O.A.S. Romero, 2001. Antimalarial activity of dihydroartemisinin derivatives against *P. falciparum* resistant to mefloquine: A quantum chemical and multivariate study. Theochem. J. Mol. Struct., 572: 35-44.

Posner, G. and C.H.J. Oh, 1992. A regiospecifically oxygen-18 labeled 1,2,4-trioxane: A simple chemical model system to probe the mechanism(s) for the antimalarial activity of artemisinin (Qinghaosu). J. Am. Chem. Soc., 114: 8328-8335.

Posner, G.H., C.H. Oh, L. Gerena and K.M. Wibur, 1992. Extraordinarily potent antimalarial compounds: new, structurally simple, easily synthesizes, tricyclic 1,2,4-Trioxanes. J. Med. Chem., 35: 2459-2467.

Posner, G.H., S.B. Park, L. Gonzalez, D. Wang, J.N. Cumming, D. Klinedinst, T.A. Shapiro and M.D. Bachi, 1996. Evidence for the Importance of high-valent Fe=O and of a diketone in the molecular mechanism of action of antimalarial trioxane analog of artemisinin. J. Am. Chem., 118: 3537-3538.

Shoichet, B.K., R.M. Stroud, D.V. Santi, I.D. Kuntz and K.M. Perry, 1993. Structure-based discovery of inhibitors of thymidylate synthase. Science, 259: 1445-1446.

Yang, Y.Z., W. Aswamahasakda and S.R. Meshnick, 1993. Alkylation of human albumin by the antimalarial artemisinin. Biochem. Pharmacol., 46: 336-339.

Zhang, F., D.K. Jr Gosser. and S.R. Meshnick, 1992. Hemin-catalyzed decomposition of artemisinin (qinghaosu). Biochem Pharmacol., 43: 1805-1809.

Zhou, W.S. and X.X. Xu, 1994. Total synthesis of the antimalarial sesquiterpene peroxide qinghaosu and yingzhaosu. Acc. Chem. Res., 27: 211-216.